

# New findings in the catalytic activity of zinc glutarate and its application in the chemical fixation of CO<sub>2</sub> into polycarbonates and their derivatives

Moonhor Ree <sup>a,\*</sup>, Yongtaek Hwang <sup>a,1</sup>, Jong-Seong Kim <sup>a,1</sup>, Hyunchul Kim <sup>a,1</sup>,  
Gahee Kim <sup>a</sup>, Heesoo Kim <sup>b</sup>

<sup>a</sup> Department of Chemistry, National Research Lab for Polymer Synthesis and Physics, and Polymer Research Institute,  
Pohang University of Science and Technology, Pohang 790-784, Republic of Korea

<sup>b</sup> Department of Microbiology, Dongguk University College of Medicine, Gyeongju 780-714, Republic of Korea

Available online 11 April 2006

## Abstract

A heterogeneous zinc glutarate (ZnGA) catalyst and its derivatives were prepared from various zinc and glutarate sources. The hydrothermal reaction between zinc perchlorate hexahydrate and glutaronitrile afforded ZnGA single crystals (*sc*-ZnGA), with a monoclinic lattice unit cell and a *P2<sub>1</sub>/c* space group, as determined by X-ray single-crystal structural analysis. The structural details of the ZnGA catalyst are crucial in helping to elucidate its activity in the copolymerization reactions between carbon dioxide (CO<sub>2</sub>) and alkylene oxides. X-ray absorption studies provided direct evidence that CO<sub>2</sub> and propylene oxide (PO) are reversibly adsorbed onto the Zn ion centers on the ZnGA surface. Compared to CO<sub>2</sub>, PO was found to insert more easily into the Zn–O bond of the ZnGA catalyst, suggesting that the ZnGA-catalyzed copolymerization is initiated by PO rather than CO<sub>2</sub>. The activity of the ZnGA catalyst in the copolymerization of CO<sub>2</sub> and PO was found to depend on the zinc source used, and its ability to produce a catalyst of large surface area and high crystallinity ( $\geq 77\%$ ). Modification of the glutarate ligand with electron-donating or withdrawing substituents failed to enhance the ZnGA catalyst activity further, indicating that glutarate is the best ligand for the Zn metal ion to achieve a high catalytic activity in the CO<sub>2</sub> copolymerization with PO. The ZnGA-catalyzed copolymerization was further optimized to maximize the yield of alternating poly(propylene carbonate), and also extended to the terpolymerization of CO<sub>2</sub> and PO with  $\delta$ -valerolactone (VL). Terpolymers with high molecular weights and yields could be obtained by adjusting the PO/VL feed ratios. In addition, the terpolymers were found to exhibit excellent enzymatic and biological degradability.

© 2006 Elsevier B.V. All rights reserved.

**Keywords:** Zinc glutarate catalyst; Heterogeneous catalyst; Carbon dioxide/propylene oxide copolymerization; Polycarbonate; Carbon dioxide/propylene oxide/ $\delta$ -valerolactone terpolymerization; Poly(carbonate-*co*-ester); Degradability

## 1. Introduction

The observed increase in atmospheric carbon dioxide (CO<sub>2</sub>) in recent years is widely believed to be a major contributor to global warming [1–4]. Atmospheric CO<sub>2</sub> is estimated to constitute around 66% of the gases contributing to global warming [4]. Human activities annually add about 24 billion tonnes of CO<sub>2</sub> to the atmosphere, with around 22 billion tonnes of that coming from the burning of fossil fuels [5,6].

Approximately 15 billion tonnes of CO<sub>2</sub> is removed from the atmosphere by plants, soil, and the oceans, leaving a net addition of 9 billion tonnes per year [5,6]. The concentration of atmospheric CO<sub>2</sub> is therefore increasing at a rate of 1 parts per million by volume (ppmv) per year [5,6], where the present day CO<sub>2</sub> level is reported to be 345 ppmv [4–6].

Carbon dioxide (the cheapest and most abundant raw material source of carbon) [7,8], on the other hand, finds useful application in the production of polymeric materials for use in industry. A prime example of such polymeric materials is poly(alkylene carbonate), which can be produced by the copolymerization of CO<sub>2</sub> with alkylene oxide (e.g., ethylene oxide, propylene oxide, isobutylene oxide, cycloheptene oxide, cyclopentene oxide, cyclohexene oxide, and other cyclic

\* Corresponding author. Tel.: +82 54 279 2120; fax: +82 54 279 3399.

E-mail address: [ree@postech.edu](mailto:ree@postech.edu) (M. Ree).

<sup>1</sup> These authors contributed equally to this work.

oxides) [9–30]. Poly(propylene carbonate) (PPC) was reported in 1969 as the first poly(alkylene carbonate) product synthesized from CO<sub>2</sub> [9]. In this case, the reaction was catalyzed with a catalyst formed from diethyl zinc and water, to give a polymerization yield of 13.4 g polymer/g of catalyst or less. Thereafter, much effort was concentrated on developing active heterogeneous catalysts based on zinc and other metals (e.g., aluminum, chromium, cadmium, cobalt, iron, nickel, magnesium, tin, etc.). As a result, a number of heterogeneous catalysts were reported for CO<sub>2</sub>/PO copolymerization reactions [9–30].

Among the heterogeneous catalyst systems reported for the copolymerization of CO<sub>2</sub> with propylene oxide (PO) to date [26], the activities of a selection of these catalysts were recently compared [30]. Based on the copolymerization yields reported, the catalytic activity was found to decrease in the order: Zn<sub>3</sub>[Fe(CN)<sub>6</sub>]<sub>2</sub> > ZnO/glutaric acid > Zn(OH)<sub>2</sub>/glutaric acid > Mg–isoprene complex > Cr(OOCCH<sub>3</sub>)<sub>3</sub> > ZnO/adipic acid > ZnEt<sub>2</sub>/pyrogallol > ZnEt<sub>2</sub>/H<sub>2</sub>O > ZnEt<sub>2</sub>/poly(*p*-hydroxystyrene) > ZnEt<sub>2</sub>/resorcinol [30]. Although the Zn<sub>3</sub>[Fe(CN)<sub>6</sub>]<sub>2</sub> catalyst was reported to give the highest yield in the copolymerization of CO<sub>2</sub> with PO, the copolymer product was found to include a large fraction of ether linkages on the polymer backbone [27,30–32]. The Cr(OOCCH<sub>3</sub>)<sub>3</sub> catalyst was also found to provide polycarbonate products containing a large fraction of ether linkages [16,17,21]. In contrast, the ZnO/glutaric acid catalyst system (i.e., zinc glutarate (ZnGA)) produced a high yield of alternating polycarbonate.

As reviewed above, considering both copolymerization yield and copolymer composition, the ZnGA catalyst prepared from the reaction of ZnO and glutaric acid has been found to provide the most effective heterogeneous catalyst to deliver poly(alkylene carbonates) (e.g., PPC) with a reasonably high molecular weight. Moreover, this particular ZnGA catalyst is readily synthesized from cheap zinc and glutaric acid sources in excellent yield (mostly 100%), making it highly cost effective. While the maximum yield of poly(alkylene carbonate) produced in the copolymerization reaction using this ZnGA catalyst is limited to just ca. 34 g polymer/g of catalyst, the demand for this ZnGA catalyst is still substantial. Interestingly, however, no structural information has been reported for the ZnGA catalyst, making it difficult to elucidate its catalytic mechanism and activity. This lack of structural information is due in part to the difficulty of preparing single crystals of ZnGA, which results from its extremely low solubility in all common solvents. In addition, ZnGA is a heterogeneous catalyst, which requires organic solvents (e.g., acetonitrile, anisole, benzene, chlorobenzene, 1,4-dioxane, hexane, methylene chloride, etc.) to be employed as reaction media in copolymerization reactions [9–30]. Supercritical CO<sub>2</sub> was also investigated as a reaction medium, but the copolymerization yield was limited to just ca. 12 g/g of catalyst [18].

In this paper, we provide new findings regarding the heterogeneous ZnGA catalyst and its catalytic activity in the chemical insertion of CO<sub>2</sub> into polycarbonates, in particular PPC and its terpolymers with lactones.

## 2. New findings in ZnGA catalyst and its activity

### 2.1. ZnGA single-crystal preparation and its structural determination

We have attempted to make single crystals of ZnGA (*sc*-ZnGA) via optimizing reaction parameters of conventional synthesis procedures from various zinc and glutarate sources. The synthesis of *sc*-ZnGA was further attempted by hydrothermal reactions of glutaronitrile with various zinc sources such as zinc chloride, zinc oxide, zinc nitrate, and zinc acetate. The *sc*-ZnGA synthesis was also tried by hydrothermal reactions of glutaric acid with the zinc sources and zinc perchlorate hexahydrate. All these attempts, however, failed to obtain a reasonable size of *sc*-ZnGA. The hydrothermal reaction of glutaronitrile and zinc perchlorate hexahydrate only gave a large size of *sc*-ZnGA (Figs. 1 and 2) [33]. The synthesis of *sc*-ZnGA was found to be highly reproducible. The obtained *sc*-ZnGA was thermally stable up to 471 °C in nitrogen atmosphere.

The wide-angle X-ray diffraction pattern of *sc*-ZnGA in ground powder was identical to that of the commonly synthesized ZnGA in powder (Fig. 3). Further the X-ray single-crystal structure determinations found that the obtained *sc*-ZnGA is a crystal composed of monoclinic lattice unit cell with a space group of *P*2/*c* and lattice parameters of *a* = 13.934(3) Å, *b* = 4.7842(11) Å, *c* = 9.276(2) Å, and β = 90.628(5)°. All Zn ion centers of the crystal thus coordinate to four carboxyl oxygen atoms on different glutarate ligands via four *syn-anti* bridges, forming a distorted tetrahedral geometry (see Fig. 4). Here it is noteworthy that

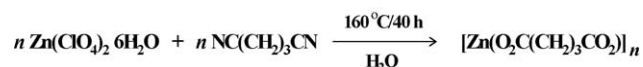


Fig. 1. Synthetic scheme of ZnGA single crystal from zinc perchlorate hexahydrate (Zn(ClO<sub>4</sub>)<sub>2</sub>·6H<sub>2</sub>O) and glutaronitrile (NC(CH<sub>2</sub>)<sub>3</sub>CN).

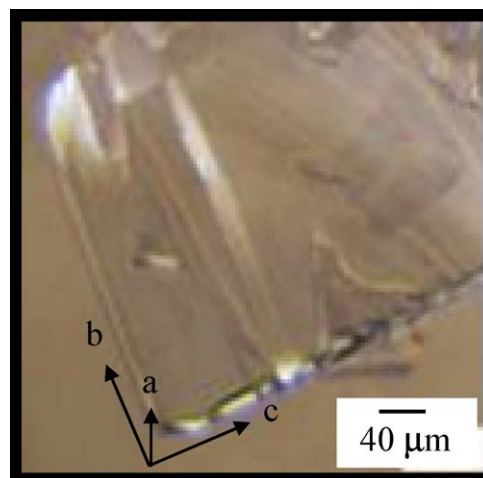


Fig. 2. Optical microscopy image of *sc*-ZnGA catalyst; the crystallographic *a*-axis is parallel to the thickness direction of the single-crystal plate.

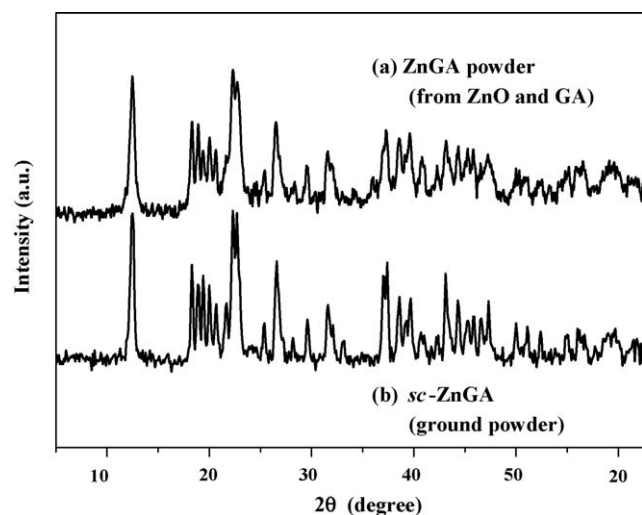


Fig. 3. X-ray diffraction patterns of ZnGA (ZnO/glutaric acid) in powder (a) and *sc*-ZnGA in ground powder (b). The Ni filtered Cu K $\alpha$  radiation source (0.15 nm wavelength) was used in the measurements.

the crystallographic *a*-axis in the single-crystal plate is parallel to the thickness direction of the crystal plate (Fig. 2). The glutarate ligands take on either a bent (type-I) or a fully extended (type-II) conformation, depending on their location in the crystal structure. Consequently, each Zn ion center coordinates with two carboxyl oxygen atoms from type-I glutarate ligands and two from type-II glutarate ligands, generating a three-dimensional network. The network structure consists of two types of metallacycles: one type is a 16-membered metallacycle (A) composed of two Zn ions [e.g., Zn(1) and Zn(4) with an interatomic distance of 6.990 Å] and two glutarate ligands in the type-I conformation and the other type is a 24-membered metallacycle (B) composed of four Zn ions [e.g., Zn(1), Zn(2), Zn(5), and Zn(6)] and two glutarate ligands in the type-II conformation as well as two carboxyl groups on two glutarate ligands in the type-I conformation. These metallacycles A and B are arranged in alternating layers along the *a*-axis (mean separation = 6.968 Å), and make eclipsed stacks along the *b*-axis, forming their own channel structures (Fig. 4b). In the case of metallacycle B channel, a small fraction of free volume is generated when the van der Waals radii of the constituent atoms are accounted for. The distance between Zn···4(O) layers in the metallacycle A channel is similar to that in the metallacycle B channel, but channel A is almost completely filled by the van der Waals radii of the constituent atoms due to the alkylenyl units of the ligands in the bent conformation. Due to these limited spaces, the carbon dioxide and alkylene oxide monomers cannot diffuse through the channels; however, the channels do give rise to a surface topology on which the monomers adsorb favorably. Overall, the coordination pattern of *sc*-ZnGA is very different from the structures commonly reported for zinc monocarboxylates, in which two zinc atoms are linked by three *syn-syn* and one *syn-anti* bridging carboxylate ligands to produce a linear(3,1) polymer [34].

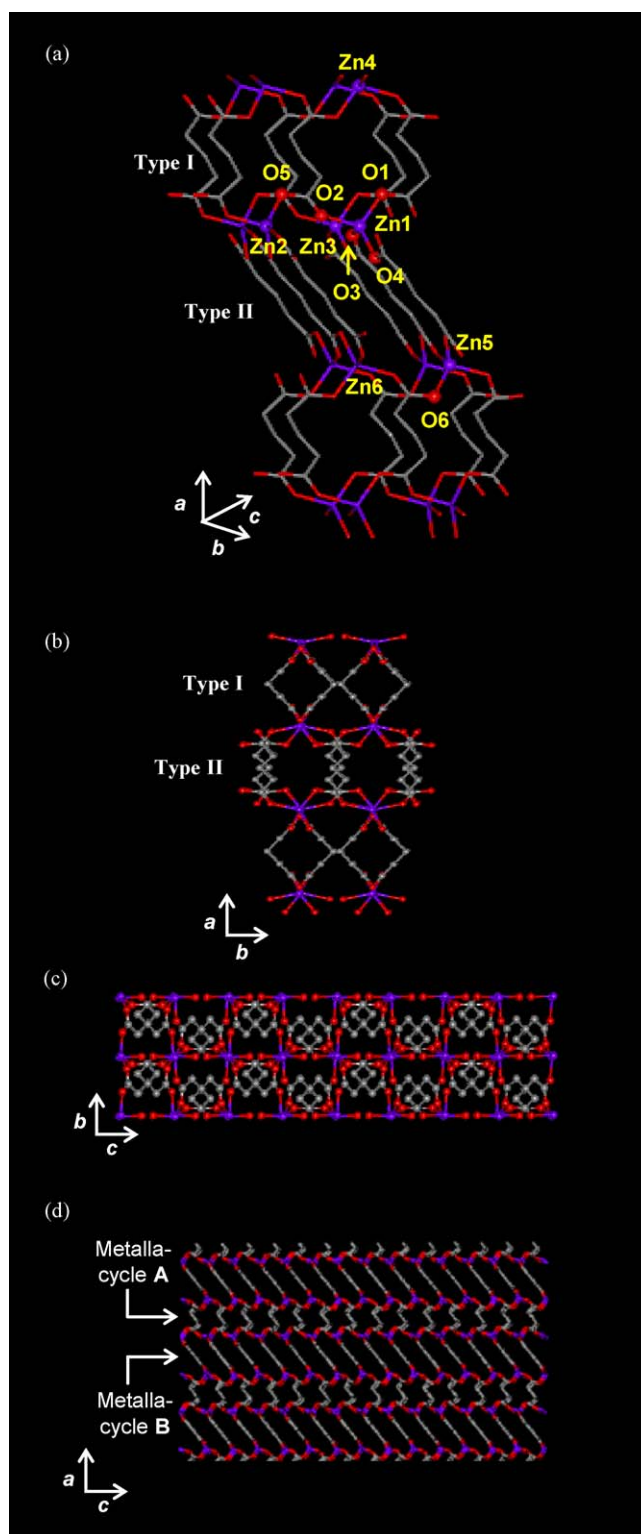


Fig. 4. Coordination geometry around the Zn cation centers in *sc*-ZnGA. (a) The atoms are denoted as Zn, O, and C. Selected bond distances (Å): Zn(1)···Zn(2) 4.639, Zn(1)···Zn(3) 4.784, Zn(1)···O(1) 1.968, Zn(1)···O(2) 1.961, Zn(1)···O(3) 1.954, Zn(1)···O(4) 1.961. View down the crystallographic (b) *c*-axis; (c) *a*-axis; (d) *b*-axis showing the packing order of two types of metallacycles resulted from the coordinations of the glutarate ligands in the bent and fully extended conformations to Zn ions: (A) 16-membered metallacycle and (B) 24-membered metallacycle.

## 2.2. Catalytic mechanism of ZnGA in CO<sub>2</sub>/PO copolymerization

Recently the surface characteristics of ZnGA catalyst (which was prepared from ZnO and glutaric acid) were first investigated by means of near edge X-ray absorption fine structure (NEXAFS) spectroscopy [35]. The surface composition of the catalyst was further examined by X-ray photoelectron spectroscopy (XPS) [35,36]. These studies found the presence of uncoordinated carboxyl groups on the surface of the catalyst. The results indicated that unsaturated zinc metal ions are present on the outermost surface of the ZnGA catalyst. Moreover, the outermost layer of the ZnGA catalyst was found to contain more hydrocarbon units than the inner layers.

With these surface characteristics of the ZnGA catalyst, we further examined catalytic adsorptions of CO<sub>2</sub> and PO on the catalyst surface using NEXAF spectroscopy [35]. These studies found the following. Adsorption of CO<sub>2</sub> and PO onto the ZnGA catalyst and insertion of these molecules into the Zn–O bond of the catalyst were detected. However, the CO<sub>2</sub> adsorbed and inserted into the ZnGA catalyst was replaced by PO treatment and vice versa, indicating that the surface state of ZnGA is changed reversibly by the final treating species (i.e., CO<sub>2</sub> or PO). This reversible adsorption and insertion of CO<sub>2</sub> and PO onto the ZnGA surface provides a clue to the mechanism by which alternating poly(propylene carbonate) is produced in the ZnGA-catalyzed copolymerization of CO<sub>2</sub> and PO. However, in comparison to CO<sub>2</sub>, PO was more easily adsorbed onto the ZnGA catalyst and inserted into the Zn–O bond. As a consequence, PO significantly modified the catalyst surface. This suggests that the ZnGA-catalyzed copolymerization is initiated by PO rather than CO<sub>2</sub> (Fig. 5).

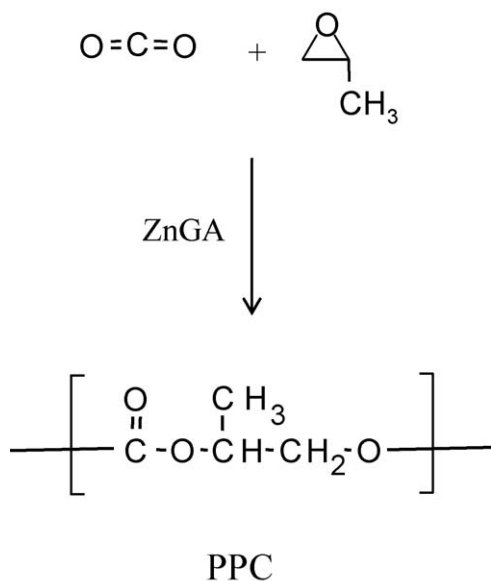


Fig. 5. Copolymerization of carbon dioxide with propylene oxide, producing poly(propylene carbonate) (PPC).

## 2.3. Effect of zinc sources in the catalytic activity of ZnGA

A series of ZnGA catalysts were prepared via the reactions of glutaric acid with either zinc hydroxide (Zn(OH)<sub>2</sub>) or diethyl zinc (ZnEt<sub>2</sub>), and glutaric anhydride with zinc nitrate hexahydrate (Zn(NO<sub>3</sub>)<sub>2</sub>·6H<sub>2</sub>O) [30]. In addition, ZnGA was also synthesized from the reaction of ZnO and glutaric acid, as described above [30]. The obtained ZnGA catalysts were examined by IR spectroscopy and X-ray diffraction. All the catalysts revealed similar IR spectra and X-ray diffraction patterns. However, their surface area and crystallinity were found to vary, depending on the zinc and glutaric source used. The surface area of the ZnGA catalysts produced from the various reactants was determined to be as follows: ZnGA (Zn(NO<sub>3</sub>)<sub>2</sub>·6H<sub>2</sub>O/glutaric anhydride) ≈ ZnGA (ZnO/glutaric acid) < ZnGA (Zn(OH)<sub>2</sub>/glutaric acid) < ZnGA (ZnEt<sub>2</sub>/glutaric acid). The crystallinity of the as-formed ZnGA catalysts, on the other hand, increased in the order: ZnGA (ZnEt<sub>2</sub>/glutaric acid) ≪ ZnGA (Zn(OH)<sub>2</sub>/glutaric acid) < ZnGA (Zn(NO<sub>3</sub>)<sub>2</sub>·6H<sub>2</sub>O/glutaric anhydride) < ZnGA (ZnO/glutaric acid).

Each of the ZnGA catalysts was tested in the CO<sub>2</sub> copolymerization with PO (Fig. 5) [30]. Here, copolymerization yields of 64 g PPC/g of catalyst for the ZnGA (ZnO/glutaric acid) system, 8.8 g for the ZnGA (Zn(OH)<sub>2</sub>/glutaric acid), 15.4 g for the ZnGA (Zn(NO<sub>3</sub>)<sub>2</sub>·6H<sub>2</sub>O/glutaric anhydride), and 2.5 g for the ZnGA (ZnEt<sub>2</sub>/glutaric acid) system were obtained (Table 1). These results indicate that the polymer yield from the CO<sub>2</sub> copolymerization with PO is strongly dependent on the synthetic history of the ZnGA catalyst, namely the zinc source used in the ZnGA synthesis.

In particular, the ZnGA (ZnO/glutaric acid) catalyst was found to produce the highest yield (64 g) in the copolymerization reaction. This yield is considered the highest among the copolymerization yields reported, and is significantly higher than the maximum yield (ca. 34 g polymer/g of catalyst) reported in the literature [28–30]. As described above, the ZnGA catalyst was revealed to have a relatively low surface area, but the highest crystallinity among the catalysts of this

Table 1  
Results of copolymerizations of CO<sub>2</sub> and PO with aids of ZnGA catalysts prepared from various zinc sources with glutaric acid and its anhydride<sup>a</sup>

ZnGA catalyst system	Copolymerization yield <sup>b</sup> (g/g of catalyst)	PPC product
		$\overline{M}_n/\overline{M}_w/\text{PDI}^c$
ZnO/glutaric acid	64.0	143k/343k/2.4
Zn(OH) <sub>2</sub> /glutaric acid	8.8	22k/65k/3.0
Zn(NO <sub>3</sub> ) <sub>2</sub> ·6H <sub>2</sub> O/glutaric anhydride	15.4	45k/315k/7.0
ZnEt <sub>2</sub> /glutaric acid	2.5	11k/124k/11.3

<sup>a</sup> Copolymerization condition: 1.0 g catalyst, 51.5 atm CO<sub>2</sub>, 100 mL PO, 60 °C, and 40 h [30].

<sup>b</sup> Yield of alternating poly(propylene carbonate) insoluble in methanol.

<sup>c</sup> Measured by gel permeation chromatography calibrated with polystyrene standards:  $\overline{M}_n$ , number-average molecular weight;  $\overline{M}_w$ , weight-average molecular weight; PDI, polydispersity index. Tetrahydrofuran (THF, HPLC grade) was used as the eluent.

study. Taking these facts into account, the crystallinity (i.e., morphological structure) of the ZnGA catalyst would appear to be a key factor in determining the catalytic activity in the CO<sub>2</sub>/PO copolymerization.

#### 2.4. Effect of glutarate sources in the catalytic activity of ZnGA

The active catalytic site in ZnGA is the Zn ion center, which coordinates four carboxyl oxygen atoms from different glutarate ligands (Fig. 4) [33,36]. This Zn ion center is a Lewis acid, the characteristics of which are expected to change when an electron-donor or withdrawing substituent is incorporated into the glutarate ligand. Any changes in the Lewis acidic characteristics of the Zn ion center may directly influence the catalytic activity in the CO<sub>2</sub>/PO copolymerization.

Therefore, a series of ZnGA derivatives were synthesized from the reactions of ZnO with various glutaric acid derivatives: 2,2-dimethylglutaric acid (2,2-DMGA), 3,3-dimethylglutaric acid (3,3-DMGA), 2-methylglutaric acid (2-MGA), 3-methylglutaric acid (3-MGA), 3-phenylglutaric acid (3-PhGA), 2-ketoglutaric acid (2-KetoGA), 3-ketoglutaric acid (3-KetoGA), 3,3-tetramethyleneglutaric acid (3,3-TMGA), mono-methyl glutarate (mono-MGA), and glutaric acid [37]. An additional zinc catalyst was also prepared from the reaction of ZnO and diglycolic acid (DGCA) [37]. These catalysts were tested in the CO<sub>2</sub> copolymerization with PO [37], the results of which are shown in Table 2.

As can be seen in Table 2, all of the as-formed ZnGA catalysts produced PPC in the copolymerization reaction, albeit with relatively low molecular weights and yields (0.02–7.80 g/g of catalyst) compared to those produced using the ZnGA (ZnO/glutaric acid) catalyst.

Table 2  
Results of copolymerizations of CO<sub>2</sub> and PO with aids of ZnGA derivative catalysts prepared from ZnO with various glutarate derivatives<sup>a</sup>

ZnGA derivative catalyst system	Copolymerization yield (g/g of catalyst) <sup>b</sup>	PPC product
		$\overline{M}_n/\overline{M}_w/\text{PDI}^c$
ZnO/glutaric acid	64.0	143k/343k/2.4
ZnO/2,2-DMGA	0.02	–
ZnO/3,3-DMGA	0.60	14k/166k/11.7
ZnO/2-MGA	0.04	12k/62k/5.2
ZnO/3-MGA	1.17	37k/285k/7.7
ZnO/3-PhGA	0.02	22k/180k/8.2
ZnO/2-KetoGA	0.10	8k/48k/5.5
ZnO/3-KetoGA	0.02	11k/52k/4.4
ZnO/3,3-TMGA	0.11	15k/104k/6.6
ZnO/mono-MGA	7.80	23k/82k/3.5
ZnO/DGCA	2.90	32k/202k/6.1

<sup>a</sup> Copolymerization condition: 1.0 g catalyst, 51.5 atm CO<sub>2</sub>, 100 mL PO, 60 °C, and 40 h [40].

<sup>b</sup> Yield of alternating poly(propylene carbonate) insoluble in methanol.

<sup>c</sup> Measured by gel permeation chromatography calibrated with polystyrene standards:  $\overline{M}_n$ , number-average molecular weight;  $\overline{M}_w$ , weight-average molecular weight; PDI, polydispersity index. Tetrahydrofuran (THF, HPLC grade) was used as the eluent.

The copolymerization results indicate that all of the substituents considered here suppress the catalytic activity of ZnGA (ZnO/glutaric acid) to a large extent. This is understood when considering several aspects of the catalysts as follows. First, the introduction of electron-donating substituents into glutaric acid results in an increase in the nucleophilicities of the carboxylic acids, whereas incorporation of electron-withdrawing groups results in a decrease in nucleophilicity. These changes in the nucleophilicities of the carboxylic acids have an undesirable effect on the Lewis acidity of the zinc metal ion in the coordination compound. Second, the side group substituents on the ZnGA catalyst generate steric hindrance around the centered zinc metal ion, consequently lowering the catalytic activity towards the monomers. Therefore, the low catalytic activities of the zinc catalyst derivatives may be due to the electronic and steric effects of the substituents, which may change the coordination characteristics of the carboxylates to the zinc metal ion. Finally, with the exception of the ether linkage of DGCA, all of the substituents add additional bulk around the active Zn ion center, influencing the morphological structure of the catalyst, which may give rise to a reduction in the catalytic activity.

#### 2.5. Effect of copolymerization conditions in the catalytic activity of ZnGA

According to previous studies [9–30], both the yield and molecular weight of the polymer product in the CO<sub>2</sub>/PO copolymerization reaction are dependent on CO<sub>2</sub> pressure, temperature, and reaction time. In general, both the yield and molecular weight increase with increasing CO<sub>2</sub> pressure up to 15–20 atm, and then level off with further increases in the CO<sub>2</sub> pressure. The yield also increases with increasing temperature, but levels off around 60 °C, whereas the molecular weight drops with increasing temperature. Increasing the reaction time also causes increases in the yield and molecular weight. The yield increases with reaction time up to about 40 h and then levels off. By contrast, the molecular weight increases with increasing reaction time, reaches to a maximum, and then decreases with further increase of the reaction time. Taking these facts into account, we have attempted to optimize the ZnGA (ZnO/glutaric acid) catalyzed copolymerization of CO<sub>2</sub> and PO by varying the catalyst and comonomer loadings, and by altering the reaction temperature and time [30]. All copolymerizations were conducted in bulk without the use of organic solvents (Fig. 5). Representative results are summarized in Table 3.

As can be seen in Table 3, the copolymerization yield is strongly dependent on the amount of PO loading per gram of catalyst under a pressure of 51.5 atm CO<sub>2</sub>, at a given reaction temperature and time (60 °C and 40 h); the PO loading of 100 mL/g of catalyst gave the highest polymer yield. To determine the minimum reaction time that still gave acceptably high yields, the copolymerization was performed at varying reaction times between 16 and 40 h, under a CO<sub>2</sub> pressure of 51.5 atm and a fixed temperature 60 °C. Overall, the polymer yield was found to increase with increasing reaction time,

Table 3

Results of the ZnGA (ZnO/glutaric acid) catalyzed copolymerizations of CO<sub>2</sub> and PO in various conditions

Copolymerization condition <sup>a</sup>			Copolymerization yield <sup>b</sup> (g/g of catalyst)	PPC product	
PO (mL)	T (°C)	t (h)		$\overline{M}_n/\overline{M}_w/\text{PDI}^c$	$[\eta]^d$
24	60	40	14.5	120k/355k/3.0	–
39	60	40	36.7	138k/363k/2.6	–
50	60	40	44.5	–	0.577
60	60	40	45.8	–	0.905
75	60	40	54.6	–	0.746
100	60	40	64.0	143k/343k/2.4	0.988
150	60	40	43.7	–	1.243
200	60	40	41.9	–	0.644
100	60	32	57.0	136k/345k/2.5	–
100	60	24	34.0	–	–
100	60	16	29.0	–	–
1000 <sup>e</sup>	60	40	70.0	210k/265k/1.3	–

<sup>a</sup> Copolymerization condition: 1.0 g catalyst, 51.5 atm CO<sub>2</sub> [30].

<sup>b</sup> Yield of alternating poly(propylene carbonate) insoluble in methanol.

<sup>c</sup> Measured by gel permeation chromatography calibrated with polystyrene standards:  $\overline{M}_n$ , number-average molecular weight;  $\overline{M}_w$ , weight-average molecular weight; PDI, polydispersity index. Tetrahydrofuran (THF, HPLC grade) was used as the eluent.

<sup>d</sup> Intrinsic viscosity measured by viscometry in benzene at 35.0 °C using a Ubbelohde viscometer.

<sup>e</sup> 10.0 g catalyst and 25.7 atm CO<sub>2</sub> were used.

reaching the highest yield (64 g polymer/g of catalyst) after 40 h. Consequently, a reduction in reaction time to below 40 h caused a sacrifice in the polymer yield. Further, the copolymerization reaction was investigated by varying the reaction temperature over the range above and below 60 °C, and by increasing the reaction time beyond 40 h. However, no further increase in the yield of the alternating PPC product was achieved. For CO<sub>2</sub>/PO copolymerizations with the optimized condition, the polymer product insoluble in methanol was obtained with >99% of the total yield. This indicates that in the copolymerization, the homopolymers of PO are not made, the products that contain ether linkages on the polymer backbone, and the cyclic carbonate byproducts, which are soluble in methanol; otherwise, they might be obtained only in very small quantities.

In addition, the copolymerization reaction was scaled up 10-fold to 1000 mL of PO, while maintaining a ratio of 100 mL PO/g of catalyst. Here, CO<sub>2</sub> could not be pressurized to the 51.5 atm employed in the relatively small-scale copolymerization reaction, such that a lower CO<sub>2</sub> pressure of 25.7 atm was employed instead. This resulted in an increased yield of alternating PPC product (70 g/g of catalyst); the polymer yield is improved by 9.4%, compared to that of the copolymerization reaction involving a 100 mL PO loading (Table 3). In addition, the molecular weight of the PPC product was found to be greater, and the polydispersity narrower, compared to the PPC prepared on the smaller scale. Overall, the scale-up in the polymerization was very successful.

In conclusion, we have determined the following optimized process conditions for the ZnGA-catalyzed copolymerization of CO<sub>2</sub> and PO, which do not need additional solvents: 100 mL

PO loading per gram of catalyst, 25–52 atm CO<sub>2</sub>, 60 °C, and 40 h. This optimized process results in an improved polymer yield for large-scale copolymerization reactions. Moreover, this optimized ZnGA-catalyzed copolymerization only produced alternating copolymer PPC.

This copolymerization process was found to further enhance the yield of PPC product when fine powdery ZnGA (ZnO/glutaric acid) catalyst (0.2–0.3 μm) was used in the copolymerization [38].

## 2.6. Morphological structure modification and its effect in the catalytic activity of ZnGA

As mentioned above, the ZnGA (ZnO/glutaric acid) catalyst is always prepared with a size of 1–10 μm in the synthesis; this catalyst revealed a high crystallinity but a low surface area. In general, the catalytic activity of a heterogeneous catalyst depends on the crystal habit, particle size and size distribution, impurities, and content of polymorphous modification. Taking these general facts into account, ZnGA (ZnO/glutaric acid) catalyst needs to be prepared in the best way to significantly increase its surface area with keeping the high crystallinity.

Recently, it was reported that the external morphologies and/or crystalline structures of inorganic particles, such as calcium carbonate, calcium phosphate, and zinc oxide, can be significantly changed by using organic templates in the synthesis [39,40]. For this purpose, among the organic templates reported so far, amphiphilic block copolymer was found to be advantageous because of the functionalities and well-controlled compositions and lengths of its blocks [39,40]. Regarding the functionalities of such amphiphilic template, one block is known to adsorb to the surface of solid particle (so-called ‘anchor block’) while the other block forms a swollen layer (so-called ‘solution block’ or ‘buoy block’) bound to the same surface via the anchor blocks [39,40]. Indeed, the solution block forms a steric shield, which can prevent the particle from agglomeration.

Therefore, we attempted to enhance the surface area of the ZnGA catalyst using a triblock copolymer (Pluronic<sup>®</sup> PE6400: poly(ethylene glycol)-*block*-poly(propylene glycol)-*block*-poly(ethylene glycol) [41]) as an amphiphilic template for the synthesis of the catalyst from zinc acetate dihydrate (Zn(OAc)<sub>2</sub>·2H<sub>2</sub>O) and glutaric acid in various reaction media: ethanol, water, and a mixture of ethanol and water (94.5/5.5, w/w) [42]. The synthesized ZnGA catalysts were characterized in terms of their surface area and surface composition as well as their particle size and morphological structure. In addition, the effects on the catalyst particle size, structure, and catalytic activity of the reaction media used in the synthesis of the catalysts were examined. Finally, the catalytic activities of the synthesized catalysts were tested in the copolymerization of CO<sub>2</sub> and PO. The results are summarized in Table 4.

The results of Table 4 provide the insights of understanding on ZnGA catalysts and their activities in the copolymerization as follows. The PE6400 template and the polarity of the solvent used as the reaction medium significantly affect the morphology, particle size, surface area, and crystallinity of the resulting

Table 4

Particle sizes and surface areas of the ZnGA ( $\text{Zn}(\text{OAc})_2 \cdot 2\text{H}_2\text{O}$ /glutaric acid) catalysts synthesized under various conditions with and without a template, Pluronic<sup>®</sup> PE6400, and their results when used in the copolymerization of  $\text{CO}_2$  with PO

Catalyst preparation <sup>a</sup>			Catalyst characterization			PPC yield <sup>c</sup> (g/g of catalyst)	PPC product $\overline{M}_n/\overline{M}_w/\text{PDI}^d$
Zinc source	Solvent	Template	Particle size ( $\mu\text{m}$ )	Surface area ( $\text{m}^2/\text{g}$ )	$X_c^b$ (%)		
ZnO	Toluene	–	5.7	19.8	95.1	64	343k/143k/2.4
$\text{Zn}(\text{OAc})_2 \cdot 2\text{H}_2\text{O}$	Ethanol/water <sup>c</sup>	–	15.5	38.0	77.8	35	335k/81k/4.2
$\text{Zn}(\text{OAc})_2 \cdot 2\text{H}_2\text{O}$	Water	PE6400	8.5	13.9	93.9	9.5	529k/51k/10.4
$\text{Zn}(\text{OAc})_2 \cdot 2\text{H}_2\text{O}$	Ethanol	PE6400	13.3	46.5	78.1	67	238k/93k/2.6
$\text{Zn}(\text{OAc})_2 \cdot 2\text{H}_2\text{O}$	Ethanol/water <sup>c</sup>	PE6400	15.3	48.5	77.6	83	160k/60k/2.7

<sup>a</sup> Reaction condition: 50 g solvent, 2.5 g (11.4 mmol)  $\text{Zn}(\text{OAc})_2 \cdot 2\text{H}_2\text{O}$ , 1.5 g (11.4 mmol) glutaric acid, 60 °C, and 10 h; in case of the template used, 2.5 g template was used [45].

<sup>b</sup> Crystallinity obtained from the measured X-ray diffraction pattern.

<sup>c</sup> Yield of alternating poly(propylene carbonate) insoluble in methanol.

<sup>d</sup> Measured by gel permeation chromatography calibrated with polystyrene standards:  $\overline{M}_n$ , number-average molecular weight;  $\overline{M}_w$ , weight-average molecular weight; PDI, polydispersity index.

<sup>e</sup> Ethanol/water = 94.5/5.5 (w/w).

ZnGA ( $\text{Zn}(\text{OAc})_2 \cdot 2\text{H}_2\text{O}$ /glutaric acid) catalyst. Further, the catalysts' surface compositions were found to be quite different from that of the ZnGA (ZnO/glutaric acid) catalyst. However, X-ray diffraction and XPS analyses found that these catalysts have the same crystal lattice unit cell structure as well as similar surface composition. These characteristics of the catalysts were found to influence the ZnGA-catalyzed copolymerizations of  $\text{CO}_2$  and PO. In particular, the ZnGA ( $\text{Zn}(\text{OAc})_2 \cdot 2\text{H}_2\text{O}$ /glutaric acid) catalyst, which was prepared in ethanol containing 5.5 wt% water using the PE6400 template, exhibited the highest catalytic activity in the copolymerization. This catalyst has a relatively large particle size of 15.3  $\mu\text{m}$  and a relatively low crystallinity  $X_c$  of only 77.6%; the  $X_c$  value is much lower than that (95.1%) of the ZnGA (ZnO/glutaric acid) catalyst. However, this catalyst revealed the largest surface area (48.5  $\text{m}^2/\text{g}$ ) despite the large particle size. The large surface area of this catalyst was found to be attributed to its wrinkled petal bundle morphology (Fig. 6). Therefore, the high catalytic activity of this catalyst might be dominated by its large surface area, and further positively supported by its reasonably high crystallinity.

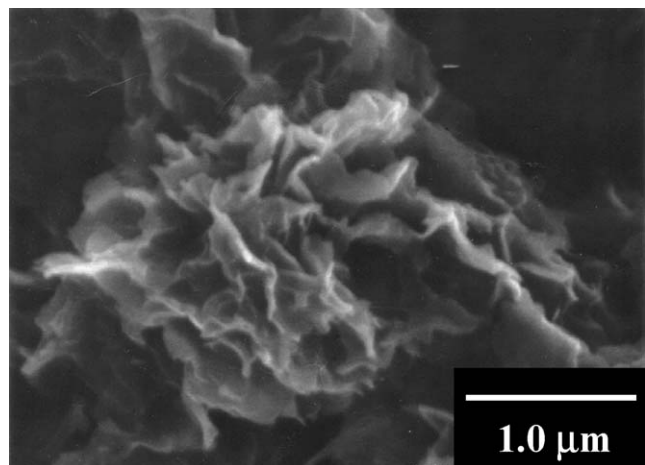


Fig. 6. SEM image of the ZnGA ( $\text{Zn}(\text{OAc})_2 \cdot 2\text{H}_2\text{O}$ /glutaric acid) catalyst prepared in ethanol/water (94.5/5.5, w/w) with PE6400.

These results along with those observed with the ZnGA (ZnO/glutaric acid) strongly suggest important information as follows. First, higher crystallinity is crucial to the activity of the catalyst in the  $\text{CO}_2$ /PO copolymerization. However, a crystallinity of ca. 77% may be enough to provide high catalytic activity to the catalyst. Second, for ZnGA catalyst with  $\geq 77\%$  crystallinity, larger surface area is critical to significantly improve the catalytic activity in the copolymerization. Finally, in the ZnGA catalyst synthesis zinc source is not limited to ZnO; any zinc source may be appropriate for the synthesis of a very active ZnGA catalyst if it can produce a catalyst of larger surface area and higher crystallinity ( $\geq 77\%$ ).

## 2.7. Extendability of ZnGA catalyst in chemical $\text{CO}_2$ fixation into terpolymers

We attempted to extend the above ZnGA-catalyzed copolymerization to the terpolymerization of  $\text{CO}_2$  and PO with an aliphatic lactone. Aliphatic polyesters prepared from lactones are presently thought to be the most attractive class of man-made polymers from the environmental standpoint, in that they degrade in contact with living tissues and in outdoor conditions [43–45]. In particular, poly( $\delta$ -valerolactone) (PVL) is biodegradable and of commercial interest because of its potential applications in biomedicine. In general, PVL is prepared by the anionic and cationic ring-opening polymerizations of  $\delta$ -valerolactone (VL). A number of catalysts have been reported for VL polymerization [45]; however, ZnGA has not yet been considered. Taking these facts into account, we aimed to chemically fix  $\text{CO}_2$  together with VL and PO into one polymer system (Fig. 7) in order to produce PPC derivatives which can reveal significantly enhanced biodegradability. This terpolymerization was performed with the aid of ZnGA catalyst for various feed ratios of these three monomers, and the chemical structures, thermal properties, and enzymatic and fungal degradabilities of the polymer products were characterized (see the experimental details in Section 4).

In this study, PO and VL were used as comonomers as well as reaction media, so no additional organic solvent was used in

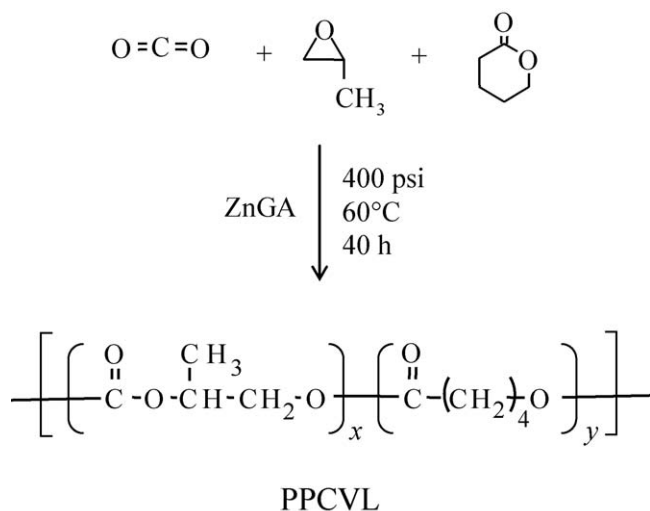


Fig. 7. Terpolymerization of carbon dioxide with propylene oxide and  $\delta$ -valerolactone, producing poly(propylene carbonate-co- $\delta$ -valerolactone) (PPCVL).

the terpolymerization, resulting in the production of no organic solvent waste. The polymer products of this terpolymerization process were found to be highly soluble in PO and VL, confirming the appropriateness of the use of PO and VL as both comonomers and reaction media. The terpolymerizations of  $\text{CO}_2$ , PO, and VL were conducted in various compositions. The results of the terpolymerizations are summarized in Table 5.

As shown in Table 5, the polymer products were synthesized with reasonably highly molecular weights; their yields ranged from 0 to 75.2 g/g of catalyst, depending on the molar feed ratio of PO and VL. In particular, the product yield was found to decrease when VL was loaded above 50 mol% with respect to the total moles of PO and VL. For each terpolymerization, the total yield of polymer product that was insoluble in methanol was >99%. This indicates that in the terpolymerization, methanol-soluble products that contain ether linkages on the polymer backbone were not made and, otherwise, obtained only in very small quantities. Further, the characteristic chemical shifts of any cyclization byproducts, which have often been observed in the copolymerization of  $\text{CO}_2$  and PO as a byproduct

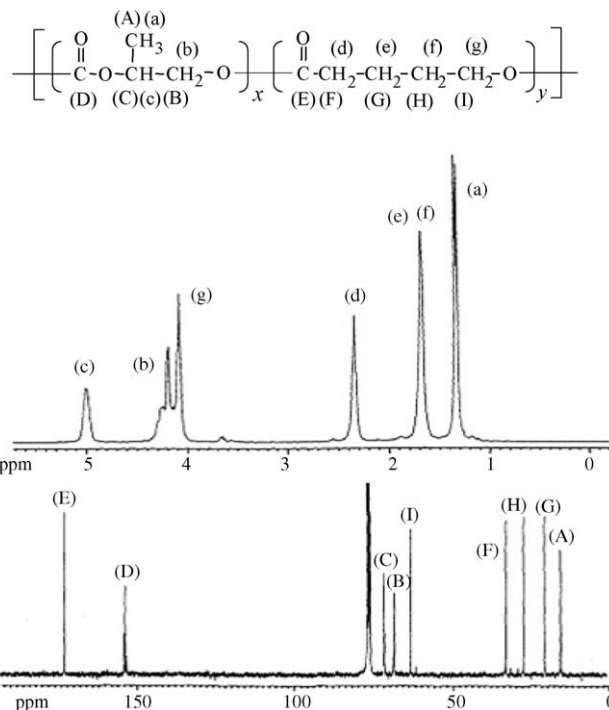


Fig. 8.  $^1\text{H}$  NMR (top) and  $^{13}\text{C}$  NMR (bottom) spectra of a poly(propylene carbonate-co- $\delta$ -valerolactone) (PPCVL(5/5)) prepared by  $\text{CO}_2$  terpolymerization with PO and VL in 5:5 feed molar ratio.

[9–27], were not detected in any of the NMR spectra obtained from the terpolymerization products. Further, no homopolymerization of VL was detected. This indicates that the ZnGA catalyst does not have any catalytic activity in the homopolymerization of VL monomer.

The chemical compositions of the methanol-insoluble polymer products were characterized using nuclear magnetic resonance (NMR) spectroscopy with proton ( $^1\text{H}$ ) and carbon ( $^{13}\text{C}$ ) probes. Fig. 8 shows representative NMR spectra, which were obtained from the polymer product PPCVL(5/5) obtained from the terpolymerization of  $\text{CO}_2$  with PO and VL with a 5:5 molar feed ratio. Fig. 9 shows the  $^1\text{H}$ – $^{13}\text{C}$  correlation two-dimensional (2D) NMR spectrum of the PPCVL(5/5) polymer product. From a detailed analysis of the 2D NMR spectrum, the NMR peaks were assigned as indexed in Figs. 8 and 9.

Table 5  
 $\text{CO}_2$  terpolymerization with PO and VL using ZnGA catalyst<sup>a</sup>

Polymer product code	PO (mL)	VL (mL)	PO/VL <sup>b</sup> (molar ratio)	Yield <sup>c</sup> (g/g of catalyst)	$\overline{M}_w$ /PDI <sup>d</sup>	$T_{g1}/T_{g2}$ ( $^\circ\text{C}$ ) <sup>e</sup>	$T_m$ ( $^\circ\text{C}$ )
PPCVL(7/3)	64	36	7/3	75.2	299k/1.61	–66/29	56
PPCVL(6/4)	53	47	6/4	67.1	161k/1.92	–59/31	57
PPCVL(5/5)	43	57	5/5	39.9	109k/2.66	–54/31	54
PPCVL(4/6)	34	66	4/6	32.5	90k/3.91	–59/31	55
PPCVL(3/7)	24	76	3/7	21.8	83k/4.15	–55/32	55
PPCVL(0/10)	0	100	0/10	None	–	–	–

<sup>a</sup> Polymerization condition: 1.00 g ZnGA (ZnO/glutaric acid), 27.2 atm  $\text{CO}_2$ , 60  $^\circ\text{C}$ , and 40 h.

<sup>b</sup> Feed molar ratio.

<sup>c</sup> Yield of PPCVL insoluble in methanol ( $\approx$ gross polymerization yield).

<sup>d</sup> Measured by gel permeation chromatography calibrated with polystyrene standards:  $\overline{M}_w$ , weight-average molecular weight; PDI, polydispersity index.

<sup>e</sup> Measured at 10.0  $^\circ\text{C}/\text{min}$  in nitrogen gas flow by DSC; glass transition temperature  $T_g$  value was determined from the onset point of glass transition; melting point  $T_m$  value was determined from the melting peak maximum.

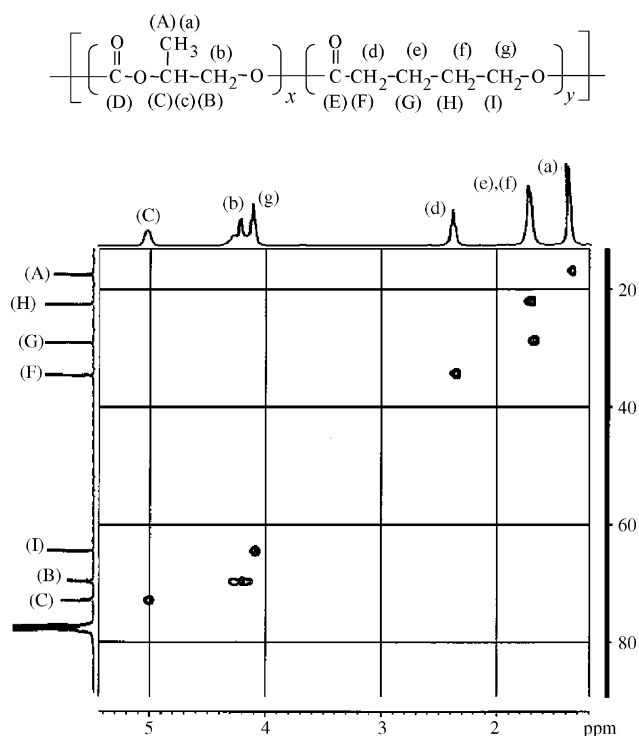


Fig. 9.  $^1\text{H}$ – $^{13}\text{C}$  correlation 2D NMR spectra of a PPCVL(5/5) terpolymer. The composition was determined to be of 61 mol% PPC and 39 mol% PVL blocks.

As can be seen in Fig. 8, each carbon atom of the PC and VL units appeared as a single peak rather than multiple peaks. These  $^{13}\text{C}$  NMR peaks are associated with the blocked PC and VL units. These NMR results collectively lead to the conclusion that in the terpolymerizations of our study, blocked PC and VL units tend to be favorably formed with long block lengths in higher populations than that of the directly linked PC–VL unit; the directly linked PC–VL unit could not be detected in the  $^{13}\text{C}$  NMR spectra because of its relatively very low population in the polymer backbone. Taking these results into account, the chemical compositions of all polymer products were estimated from the integrations of the proton NMR peaks assigned above. The results are listed in Table 6.

The  $T_g$  and  $T_m$  of the methanol-insoluble polymer products were measured using DSC; the results are summarized in Table 5. The PPC polymer containing no VL units has only a single  $T_g$ , 29 °C, indicating that the PPC polymer is amorphous.

Table 6  
Compositions of PPCVL terpolymers

Polymer product code	PO:VL (feed molar ratio)	Composition (molar fraction, %) <sup>a</sup>	
		PPC unit	PVL unit
PPCVL(7/3)	7/3	71	29
PPCVL(6/4)	6/4	52	48
PPCVL(5/5)	5/5	61	39
PPCVL(4/6)	4/6	22	78
PPCVL(3/7)	3/7	28	72

<sup>a</sup> Molar fractions of PPC and PVL units in the PPCVL product were determined by  $^1\text{H}$  NMR spectroscopy.

A PVL polymer (42k  $\overline{M}_w$ ) was prepared by the homopolymerization of VL monomer in nitrobenzene using methyl triflate as a catalyst, and was found to be a crystalline polymer with a  $T_g$  of –66 °C and a  $T_m$  of 58 °C; in general, PVL exhibits a very weak glass transition in DSC measurements, causing error in the  $T_g$  determination (data not shown in Table 5). On the other hand, all the terpolymer products reveal two glass transitions and a melting transition; one  $T_g$  appears at the range of –66 to –55 °C and another  $T_g$  shows at the range of 29–32 °C, while  $T_m$  appears at the range of 54–57 °C (Table 5). Taking the  $T_g$  and  $T_m$  results of the PPC and PVL into account, the two  $T_g$  values and the  $T_m$  value of each terpolymer product can be assigned; one  $T_g$  in the lower temperature region and the  $T_m$  value are originated from the VL units in the terpolymer backbone while another  $T_g$  in the higher temperature region is originated from the PC units. These results indicate that the terpolymers are composed of PPC and PVL blocks in the polymer backbone. The terpolymers were confirmed to have 28–71 mol% PPC blocks (i.e., 29–72 mol% PVL blocks) depending on the PO/VL feed molar ratios (Table 6).

As can be seen in Table 5, ZnGA exhibits good catalytic activity in the terpolymerization of  $\text{CO}_2$ , PO, and VL, in addition to its activity in the copolymerization of  $\text{CO}_2$  and PO, but no catalytic activity was observed in the homopolymerization of VL. Further, ZnGA can polymerize PO but not initiate the homopolymerization of  $\text{CO}_2$ . As discussed earlier, NEXAFS spectroscopy studies of ZnGA found that ZnGA reversibly reacts with  $\text{CO}_2$ , and readily reacts with PO via adsorption onto the catalyst surface and insertion into the Zn–O bond [35]. These results show that the Zn ion centers positioned at the surface function as active sites in the copolymerization of  $\text{CO}_2$  and PO. Taking these considerations into account, an anionic mechanism for the terpolymerization of  $\text{CO}_2$  with PO and VL is proposed here as follows. The nucleophilic oxygen atom of the PO monomer, which has a higher reactivity due to its high ring strain, is drawn towards the zinc metal center of the ZnGA catalyst and is then inserted into the zinc–carboxyl bond, activating the zinc metal center. In the next step, the two comonomers  $\text{CO}_2$  and VL competitively interact with the activated zinc metal center and are inserted into the growing chain. Then, PO,  $\text{CO}_2$ , and VL are all competitively added to the ZnGA catalyst and thus to the growing chain throughout the terpolymerization process. Taking into consideration the chemical compositions of the terpolymers listed in Table 6, the addition of PO seems more favorable than that of VL immediately after  $\text{CO}_2$  insertion, while the addition of VL is more favorable than that of  $\text{CO}_2$  or PO immediately after VL insertion. This situation is due to the different reactivities of the comonomers and results in the formation of blocky PC and VL units in the growing polymer chain.

The terpolymers were treated with *Pseudomonas cepacia* lipase in a 0.02 M phosphate buffer solution of pH 7.0 at 37 °C, and were found to exhibit significant weight loss depending on their composition; the terpolymers with higher VL content exhibited larger weight losses due to enzymatic degradation. Even the PPCVL(7/3) terpolymer with the lowest VL content was found to exhibit excellent enzymatic degradation, namely

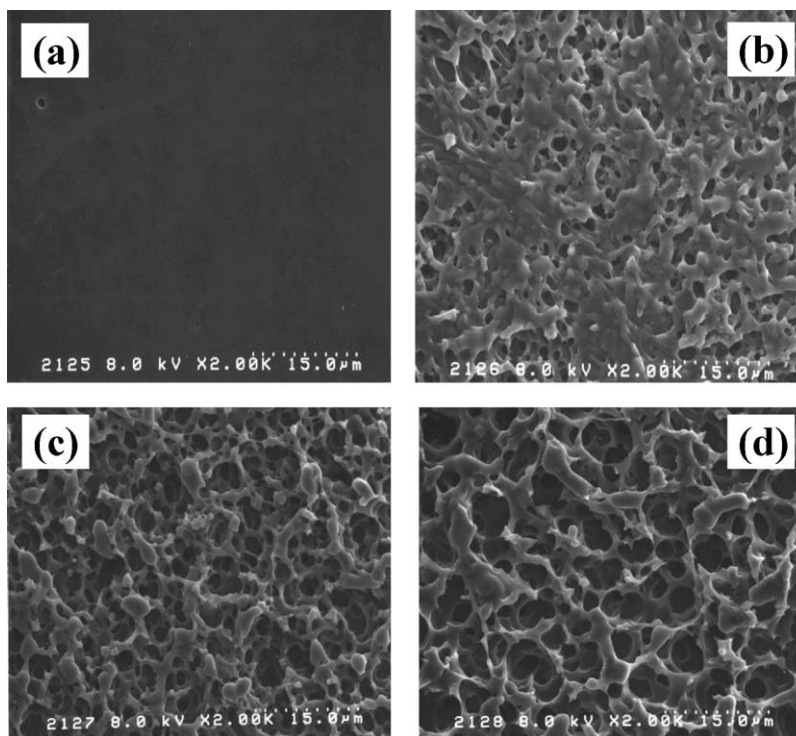


Fig. 10. Scanning electron micrographs of the PPCVL(7/3) terpolymer films before and after enzymatic degradation with *Pseudomonas* lipase: (a) before degradation; (b) after 1 day (15.6% weight loss); (c) after 2 days (29.7% weight loss); (d) after 3 days (33.9% weight loss).

34% weight loss after just 3 days' enzymatic treatment. Fig. 10 shows scanning electron microscopic images taken before and after enzymatic treatments of the terpolymer (PPCVL(7/3)) specimens; the surface erosion due to the enzymatic degradation is clearly evident in this figure. In comparison, after 3 days' enzymatic treatment the PPC polymer and the PVL homopolymer exhibited weight losses of 2 and 45%, respectively.

In addition, the terpolymers exhibited 19–32% weight loss as a result of their treatment with *Aspergillus fumigatus*, *Aspergillus terreus*, or *Penicillium olonii* in a phosphate buffer solution of pH 7.0 at 25 °C for 25 days; larger content of the VL component in the terpolymer revealed larger weight loss in the biological degradation. In comparison, after 25 days' biological treatments the PVL homopolymer exhibited a weight loss of 26–31%.

These enzymatic and biological degradabilities are comparable to those of the PVL homopolymer. In conclusion, the terpolymers were found to exhibit excellent enzymatic and biological degradability, suggesting their merit as candidate materials for biomedical applications.

### 3. Conclusions

A heterogeneous ZnGA catalyst and its derivatives were prepared from various zinc and glutarate sources. In particular, ZnGA single crystals (*sc*-ZnGA) were successfully synthesized by the hydrothermal reaction of zinc perchlorate hexahydrate and glutaronitrile, and its X-ray single-crystal structure was determined: monoclinic lattice unit cell with *P2/c* space group. The structural determination of the ZnGA catalyst is crucial to

understand the nature of its activity in the CO<sub>2</sub>/PO copolymerization reaction.

The NEXAFS and XPS studies of the ZnGA catalyst provided direct clues regarding the catalytic mechanism of ZnGA in the CO<sub>2</sub> copolymerization with PO. It was found that CO<sub>2</sub> and PO are reversibly adsorbed onto the Zn ion centers of the ZnGA surface. Compared to CO<sub>2</sub>, PO was found to be more easily adsorbed and inserted into the Zn–O bond of the ZnGA catalyst, providing sufficient evidence to suggest that the ZnGA-catalyzed copolymerization is initiated by PO rather than CO<sub>2</sub>.

The activity of the ZnGA catalyst in the copolymerization of CO<sub>2</sub> and PO was found to depend on the zinc source used in the catalyst synthesis. This zinc source dependency was attributed to the morphology differences (e.g., crystallinity and surface area) in the resulting ZnGA catalysts. However, it was determined that any zinc source can be used for the synthesis of an active ZnGA catalyst providing the resulting catalyst has a large surface area and high crystallinity ( $\geq 77\%$ ).

Enhancement of the ZnGA catalyst activity was attempted via optimization of the Lewis acidity of the Zn ion centers by incorporating an electron-donating or withdrawing substituent into the glutarate ligand. However, all of the resulting glutarate derivatives failed to achieve a better activity than that produced by the glutarate ligand itself.

The ZnGA-catalyzed CO<sub>2</sub> copolymerization with PO was optimized to maximize the yield of alternating poly(propylene carbonate) by adjusting certain reaction parameters. The optimized ZnGA-catalyzed copolymerization process was also extended to the terpolymerization of CO<sub>2</sub> and PO with the

aliphatic  $\delta$ -valerolactone (VL). The resulting PPCVL terpolymer products were synthesized in high yield and high molecular weight, depending on the PO/VL feed ratios, and found to exhibit excellent enzymatic and biological degradability, suggesting their merit as candidate materials for biomedical applications.

#### 4. Experimental

The terpolymerization of CO<sub>2</sub>, PO, and VL (see Fig. 7) was conducted with adopting a polymerization condition (i.e., catalyst loading, and reaction temperature and time) optimized previously for CO<sub>2</sub>/PO copolymerization (Section 2.5). All terpolymerizations were carried out by using a Parr autoclave reactor (500 mL) equipped with a sealed mechanical stirrer, a heating jacket, and a programmable temperature controller. Fine powdery ZnGA catalyst, which was synthesized from ZnO and GA [28,30,37], was also dried for 2 days at 100 °C in a vacuum oven ( $1 \times 10^{-5}$  Torr) just before use. The dried catalyst (1.00 g) was then added into the reactor, followed by the addition of the desired amounts of purified PO and VL using syringes in the dry box. The reactor was capped with the reactor head. The entire reactor assembly was removed from the glove box, and then pressurized with CO<sub>2</sub> to 27.2 atm after the connection pipe lines had been cleaned out with dry nitrogen gas. The reactor was heated at 60 °C with stirring. After 40 h, the reactor was cooled to room temperature, and then polymer product was removed from the reactor and dried further in a vacuum oven at room temperature, followed by weighing to determine gross yield. The dried product was dissolved in methylene chloride and transferred into a separating funnel. The catalyst residue was removed by extraction with diluted hydrochloric acid. The product solution was subsequently washed twice with distilled water, and then concentrated using a rotary evaporator. The concentrated solution was poured into excess methanol. The polymer precipitate was collected and dried in a vacuum oven at room temperature.

In order to characterize the polymer products, <sup>1</sup>H and <sup>13</sup>C NMR spectroscopy analyses were performed using a Bruker NMR spectrometer (model Aspect 300 MHz); the chemical shifts were calibrated with the chemical shifts of the chloroform-*d*<sub>1</sub> solvent. In addition, <sup>1</sup>H–<sup>13</sup>C 2D NMR spectroscopic analysis was performed. <sup>1</sup>H NMR (CDCl<sub>3</sub>):  $\delta$  = 1.3 (3H, CH<sub>3</sub>(a)), 4.2 (2H, CH<sub>2</sub>(b)), 5.0 (1H, CH(c)), 2.3 (2H, CH<sub>2</sub>(d)), 1.7 (4H, CH<sub>2</sub>(e) and CH<sub>2</sub>(f)), 4.1 (2H, CH<sub>2</sub>(g)); <sup>13</sup>C NMR (CDCl<sub>3</sub>):  $\delta$  = 16 (CH<sub>3</sub>(A)), 69 (CH<sub>2</sub>(B)), 72 (CH(C)), 154 (OCOO(D)), 173.6 (OCO(E)), 33.8 (CH<sub>2</sub>(F)), 21 (CH<sub>2</sub>(G)), 28 (CH<sub>2</sub>(H)), 64 (CH<sub>2</sub>(I)).

The weight-average molecular weight  $\overline{M}_w$  and polydispersity PDI of each polymer product were determined using a gel permeation chromatography (GPC) system (model PL-GPC 210, Polymer Labs, England) calibrated with polystyrene standards. Tetrahydrofuran (THF, HPLC grade) was used as the eluent. The glass transition temperature  $T_g$  and melting temperature  $T_m$  were measured using a differential scanning calorimeter (model DSC-220CU, Seiko, Japan); a heating rate

of 10.0 °C/min was employed and dry nitrogen gas was purged at a flow rate of 100 mL/min.

Films of the synthesized polymer products were prepared by compression molding at 120 °C for 5–10 min under a pressure of 100 kg/cm<sup>2</sup> and subsequent quenching with liquid nitrogen; the films were determined to have a thickness of 0.3 mm. The films were dried for 3 days in vacuum at room temperature before use.

For the polymer films, enzymatic degradation studies were carried out at 37 °C in a 0.02 M phosphate buffer solution (pH 7.0) containing *P. cepacia* lipase (30 units/mg) purchased from Sigma Company (USA); a sodium azide solution (2.0 wt%) was used to prevent the activities of other micro-organisms. Each buffer solution containing several pieces of polymer film weighed precisely in a test tube was incubated in an incubator at 37 °C; each solution was shaken on a shaker in the incubator during the incubation. After a determined period of time, the films were taken out from the buffer solution, washed with distilled water, and then dried in vacuum at room temperature until a constant weight was reached. The dried films were again weighed precisely to determine their weight losses with respect to their original weights, and their surface morphologies were investigated with a scanning electron microscope (SEM; model S-570, Hitachi, Japan) after coating them with gold. To evaluate the biodegradability of the terpolymer films, three kinds of fungi that had been isolated from soil in Korea, tested for their affinity with aliphatic polyester, and subsequently identified as *A. fumigatus*, *A. terreus*, and *P. olonii* were used [46]. The terpolymer films (1 cm × 1 cm) were irradiated with ultraviolet light (254 nm wavelength) at 0.13 J/cm<sup>2</sup> and incubated with the fungal suspension in 50 mL sterile inorganic salt solution at 25 °C for 25 days, as described elsewhere [46]. After incubation, the polymer films were washed with distilled water and dried in a vacuum at 25 °C to a constant weight.

#### Acknowledgements

This study was supported by the Korea Science and Engineering Foundation (National Research Lab Program: Contract No. 2005-01385), by the Ministry of Education (BK21 Program), and by POSCO.

#### References

- [1] G.A. Meehl, W.M. Washington, *Nature* 382 (1996) 56.
- [2] W.S. Broecker, *Science* 278 (1997) 1582.
- [3] K. Kacholia, R.A. Reck, *Climate Change* 35 (1997) 53.
- [4] M. Hanschild, H. Wenzel, *Environmental Assessment of Products*, vol. 2, Chapman Hall, London, 1997.
- [5] J.W. Hill, D.K. Kolb, *Chemistry for Changing Times*, seventh ed., Prentice Hall, Englewood, NJ, 1995.
- [6] J.T. Houghton, B.A. Callander, S.K. Varney (Eds.), *Climate Change 1992 (The Supplementary Report to the IPCC Scientific Assessment)*, Cambridge University, Cambridge, 1992.
- [7] J. Paul, C.M. Pradier (Eds.), *Carbon Dioxide Chemistry: Environmental Issues*, Royal Society of Chemistry, Cambridge, 1994.
- [8] M. Aresta, G. Forti, *Carbon Dioxide as a Source of Carbon*, Reidel, Dordrecht, 1986.

- [9] S. Inoue, H. Koinuma, T. Tsuruta, *J. Polym. Sci.: Polym. Lett. Ed.* 7 (1969) 287.
- [10] S. Inoue, *Chemtech*, September 1976, p. 588.
- [11] W. Kuran, in: J.C. Salamone (Ed.), *Polymeric Materials Encyclopedia*, CRC, New York, 1996, p. 6623.
- [12] D.J. Darensbourg, M.W. Holtcamp, *Coord. Chem. Rev.* 153 (1996) 155.
- [13] K. Soga, E. Imai, I. Hattori, *Polym. J.* 13 (1981) 407.
- [14] W. Kuran, S. Pasynkiewicz, J. Skupinska, A. Rokicki, *Makromol. Chem.* 177 (1976) 11.
- [15] L.-B. Chen, H.-S. Chen, J. Lin, *J. Macromol. Sci. Chem.* A24 (1987) 253.
- [16] S. Inoue, *Prog. Polym. Sci. Jpn.* 8 (1982) 1.
- [17] K. Soga, K. Uenishi, S. Hosoda, S. Ikeda, *Makromol. Chem.* 178 (1977) 893.
- [18] D.J. Darensbourg, N.W. Stafford, T. Katsurao, *J. Mol. Catal.* 104 (1995) L1.
- [19] T. Aida, M. Ishikawa, S. Inoue, *Macromolecules* 19 (1986) 8.
- [20] S. Inoue, *J. Macromol. Sci. Chem.* A25 (1988) 571.
- [21] K. Soga, K. Uenishi, S. Ikeda, *J. Polym. Sci.: Polym. Chem. Ed.* 17 (1979) 415.
- [22] X. Chen, Z. Shen, Y. Zhang, *Macromolecules* 24 (1991) 5305.
- [23] C.-S. Tan, T.-J. Hsu, *Macromolecules* 30 (1997) 3147.
- [24] D.J. Darensbourg, M.W. Holtcamp, *Macromolecules* 28 (1995) 7577.
- [25] T. Listos, W. Kuran, R. Siwec, *J. Macromol. Sci. Pure Appl. Chem.* A32 (1995) 393.
- [26] A. Rokicki, W. Kuran, *J. Macromol. Sci. Rev. Macromol. Chem.* C21 (1981) 135.
- [27] W.J. Kruper Jr., D.J. Swart, US Patent No. 4,500,704, February 19, 1985.
- [28] M. Ree, J.Y. Bae, J.H. Jung, T.J. Shin, *Korea Polym. J.* 7 (1999) 333.
- [29] J.H. Jung, M. Ree, T. Chang, *J. Polym. Sci.: Polym. Chem.* 37 (1999) 3329.
- [30] M. Ree, J.Y. Bae, J.H. Jung, T.J. Shin, *J. Polym. Sci.: Polym. Chem. Ed.* 37 (1999) 1863.
- [31] B. Lee, J.H. Jung, M. Ree, *Macromol. Chem. Phys.* 201 (2000) 831.
- [32] B. Lee, M. Ree, unpublished results.
- [33] J.-S. Kim, H. Kim, M. Ree, *Chem. Mater.* 16 (2004) 2981.
- [34] W. Clegg, D.R. Harbron, C.D. Homan, P.A. Hunt, I.R. Little, B.P. Staughan, *Inorg. Chim. Acta* 186 (1991) 51.
- [35] J.-S. Kim, M. Ree, S.W. Lee, Y.-T. Hwang, S. Baek, B. Lee, T.J. Shin, H.C. Kim, K.J. Kim, B. Kim, J. Luning, *J. Catal.* 218 (2003) 386.
- [36] J.-S. Kim, M. Ree, T.J. Shin, O.H. Han, S.J. Cho, Y.-T. Hwang, J.Y. Bae, J.M. Lee, R. Ryoo, H. Kim, *J. Catal.* 218 (2003) 209.
- [37] M. Ree, J.Y. Bae, J.H. Jung, T.J. Shin, Y.-T. Hwang, T. Chang, *Polym. Eng. Sci.* 40 (2000) 1542.
- [38] Y.Z. Meng, L.C. Du, S.C. Tiong, Q. Zhu, A.S. Hay, *J. Polym. Sci.: Part A: Polym. Chem.* 40 (2002) 3579.
- [39] H. Cölfen, *Macromol. Rapid Commun.* 22 (2001) 219.
- [40] C.-S. Yang, D. Awschalom, G. Stucky, *Chem. Mater.* 14 (2002) 1277.
- [41] Technical Report of Pluronic, 2000, BASF Company, Ludwigshafen, Germany.
- [42] J.-S. Kim, H. Kim, J. Yoon, K. Heo, M. Ree, *J. Polym. Sci.: Part A: Polym. Chem.* 43 (2005) 4079.
- [43] G. Scott, D. Gilead, *Degradable Polymer*, Chapman, London, 1995.
- [44] I. Arvanitoyannis, *Rev. Macromol. Chem. Phys.* C39 (1999) 205.
- [45] H.R. Kricheldorf, *Handbook of Polymer Synthesis*, Marcel-Dekker, New York, 1992.
- [46] H.J. Kang, T.W. Park, Y.T. Lim, *Polym. (Korea)* 20 (1996) 960.